Spin dynamics of isoelectronic bound excitons in ZnO

S. L. Chen, W. M. Chen, and I. A. Buyanova*

Department of Physics, Chemistry and Biology, Linköping University, 58183 Linköping. Sweden
(Received 28 March 2014; revised manuscript received 28 May 2014; published 10 June 2014)

Time-resolved optical spin orientation is employed to study spin dynamics of I^* and I_1^* excitons bound to isoelectronic centers in bulk ZnO. It is found that spin orientation at the exciton ground state can be generated using resonant excitation via a higher lying exciton state located at about 4 meV from the ground state. Based on the performed rate equation analysis of the measured spin dynamics, characteristic times of subsequent hole, electron, and direct exciton spin flips in the exciton ground state are determined as being $\tau_h^s = 0.4$ ns, $\tau_e^s \geqslant$ 15 ns, and $\tau_{eh}^s \geqslant 15$ ns, respectively. This relatively slow spin relaxation of the isoelectronic bound excitons is attributed to combined effects of (i) weak e-h exchange interaction, (ii) restriction of the exciton movement due to its binding at the isoelectronic center, and (iii) suppressed spin-orbit coupling for the tightly bound hole.

I. INTRODUCTION

There is considerable current interest in ZnO, a II-VI semiconductor which has a wide bandgap of 3.37 eV and a large exciton binding energy of 60 meV that are considered as key properties for applications in ultraviolet (UV) optoelectronic and white light emitting devices (for a review, see e.g. Refs. [1–3]). Besides the prominent optical performance, ZnO is also a promising material for spin-functional electronic devices and spin-based quantum computation. First of all, when alloyed with transition metals, it has been shown to exhibit ferromagnetic properties at and above room temperature (RT) [4–6] desirable for generation of spin-polarized free carriers. Secondly, ZnO is believed to have favorable spin dynamics as a weak spin-orbit interaction in this material should suppress spin relaxation mechanisms involving spin-orbit coupling such as Dyakonov-Perel mechanism [7] or Elliot-Yaffet mechanisms [8,9]. Moreover, since both zinc and oxygen atoms have a high natural abundance (around 95% and 99%, respectively) of nuclear-spin free isotopes, spin relaxation via electron-nuclear hyperfine coupling should also be strongly suppressed.

Experimentally, studies of spin dynamics in ZnO have so far been carried out for effective-mass electrons and holes that were either free or localized at shallow donors. Relatively long spin-coherence times, 1–25 ns at 4 K and 0.19 ns at RT, were measured for free and donor-bound electrons in bulk and epitaxial ZnO, from time-resolved Faraday rotation [10] and spin noise spectroscopy [11]. An even longer spin coherence time of 25 ns was reported by Liu *et al.* [12] for electrons in n-type colloidal quantum dots based on electron paramagnetic resonance spectroscopy. Effective-mass holes have been found to exhibit significantly faster spin relaxation, i.e. 100 ps at 4 K in bulk ZnO and 350 ps in strained epilayers, based on time-resolved optical orientation [13] and magneto-optical [14,15] measurements. These studies were, however, limited to holes in the neutral donor bound exciton (BX) complexes due to difficulties in fabrication of a stable p-type material of reasonable quality.

As to spin dynamics of electron-hole pairs in a form of excitons that is relevant, e.g. to optoelectronic applications, the information available so far is very limited. It has solely been restricted to free excitons (FXs) where extremely fast

(<10 ps at 4 K) spin relaxation was concluded based on the lack of FX polarization in optical orientation measurements [13]. Recently, we have shown [16] that excitons in ZnO may also be bound to isoelectronic centers forming isoelectronic bound excitons (IBXs). These isoelectronic centers have a hole attractive potential which leads to tight binding of the hole within the IBX complex and to partial quenching of its orbital angular momentum. Implications of such an electronic structure on exciton spin dynamics are currently not known and will be addressed in this paper by employing time-resolved optical spin orientation spectroscopy.

II. SAMPLES AND METHODS

Bulk single crystals investigated in this study include undoped c-plane ZnO from Cermet Inc. and c-plane ZnO implanted with hydrogen from EaglePicher Technologies. Optical measurements were performed within a temperature range of 5–30 K inside a cryofree cryostat. A wavelength tunable, pulsed Ti:Sapphire laser with a repetition rate of 76 MHz was used as an excitation source. The temporal and spectral widths of the excitation pulses were 2 ps and 1.3 meV, respectively. Transient photoluminescence (PL) was detected by a streak camera system combined with a 0.5-m single grating monochromator. Circular polarization of the excitation beam in optical spin orientation experiments was produced by a $\lambda/4$ plate in combination with a linear polarizer. The same selection of polarization optics was also used to determine a circular polarization degree of PL. The latter is defined in percentage by $P_c = 100(I^+ - I^-)/(I^+ + I^-)$, where I^+ and I^- denote the intensities of σ^+ and σ^- polarized PL, respectively. Both excitation and detection directions coincided with the direction of the c axis in ZnO.

III. EXPERIMENTAL RESULTS AND DISCUSSION

A. Optical orientation

Typical PL spectra measured at 5 K from the Cermet (the solid curve) and EaglePicher (the dashed curve) ZnO are shown in Fig. 1. In both materials, the low temperature PL spectra are dominated by sharp BX transitions. The majority of these lines originate from BX bound to either neutral ($D^0 X$) or ionized ($D^+ X$) donors. The former include PL lines related
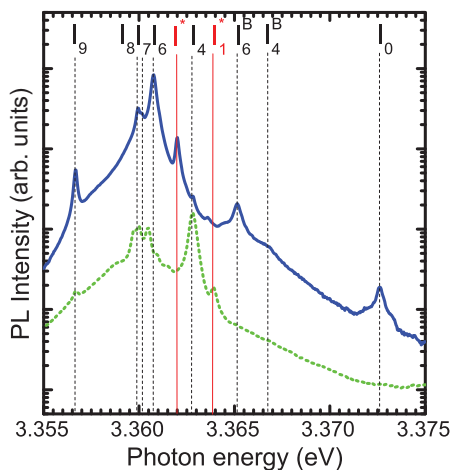
FIG. 1. (Color online) Photoluminescence spectra measured at 5 K from the Cermet (upper curve) and EaglePicher (lower curve) ZnO. Donor bound excitons are marked by the dashed vertical lines, whereas the I^* and I_1^* isoelectronic BXs are marked by the solid vertical lines.

to D^0X involving a hole from either A- or B-valence subbands and are labeled as I_4, I_6–I_9, or I_4^B and I_6^B, respectively [17–19]. D^+X gives rise to a weak transition labeled as I_0, following the notations from the literature [17,18]. In addition to the aforementioned donor bound excitons, the spectra contain PL lines labeled as I^* and I_1^* that are most pronounced for the Cermet and EaglePicher ZnO, respectively. Our previous magneto-optical measurements have proved that these transitions belong to a new class of excitons in ZnO, i.e. excitons bound at isoelectronic centers with a hole-attractive local potential [16].

In order to understand spin properties of this class of excitons, optical orientation experiments were performed. In such experiments, a chosen spin orientation of excitons may be generated by the corresponding circularly polarized excitation light. In wurtzite semiconductors, such as ZnO, combined effects of crystal field and spin-orbit interactions lead to a splitting of the valence band (VB) states into the so-called A, B, and C subbands. In a measurement configuration where light propagates along the c axis of the crystals (i.e. $k\|c$), the selection rules allow optical transitions between the conduction band states of the Γ_7 symmetry and the A (Γ_7) and B (Γ_9) VB states [20]. Since, the A- and B-valence states are constructed from the VB states with the total (spin + orbital) angular momentum projection $J_{h,z} = \pm 1/2$ and $\pm 3/2$, respectively, absorption of the circularly polarized light due to the A → CB and B → CB transitions will generate opposite spin orientations of the CB electrons. The same also applies to the corresponding FX. Therefore, in order to optically polarize the exciton spin, the excitation energy of the circular-polarized (e.g. σ^-) light in our experiments was tuned below the B-free exciton (FX$_B$). The results from the optical orientation measurements of I^* and I_1^* are summarized in Figs. 2(a) and 2(b), respectively. It was found that such excitation indeed causes circular polarization of the time-integrated I^* and I_1^* emissions and that the generated P_c critically depends on the excitation energy ($h\nu_{exc}$). This can be seen from the right part
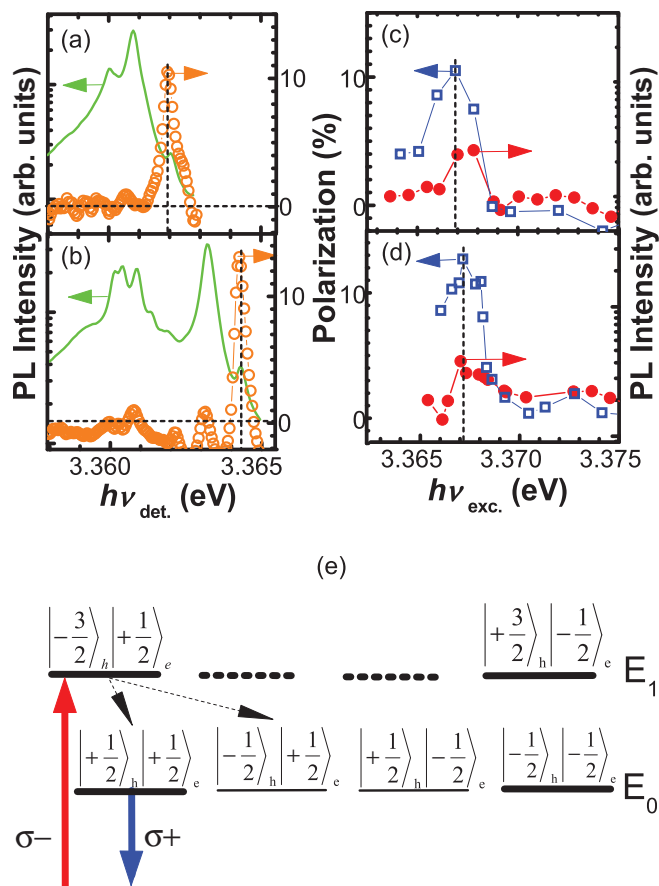

FIG. 2. (Color online) Spectral dependences of the PL circular polarization P_c (open circles) measured as a function of emission photon energy from the (a) Cermet and (b) EaglePicher ZnO. The excitation photon energy $h\nu_{exc}$ is fixed at E_1, marked by the vertical dashed line in (c) and (d), at which the maximum value of P_c is obtained for each IBX. Also shown are respective time-integrated PL spectra (solid curves) measured under linear laser excitation with the same $h\nu_{exc}$. (c) and (d) show the spectral dependences of the PL circular polarization P_c (the open squares) measured as a function of excitation photon energy from the Cermet and EaglePicher ZnO, respectively, by detecting at the peak positions of the I^* and I_1^* exciton, i.e. E_0 of the IBX as marked by the vertical dashed line in (a) and (b). The corresponding excitation spectra of the PL intensity are shown by the filled circles. (e) Schematic energy structure of an isoelectronic BX. The energy structure of the exciton ground state E_0 is taken from Ref. [16]. E_1 denotes the exciton excited state. The solid arrows represent optical absorption and emission transitions which lead to the detected σ^+ polarization under optical orientation with the σ^--polarized excitation light. The dotted arrows denote energy relaxation processes that preserve electron spin orientation within the IBX.

of Fig. 2 where the measured P_c (the open squares) is plotted as a function of $h\nu_{exc}$. It is obvious that P_c is resonantly enhanced and reaches the maximum value of $+10$ ($+13$)% for I^* (I_1^*) when $h\nu_{exc}$ is tuned at about 4 meV above the emission energy, i.e. at 3.3668 (3.3673) eV, but becomes negligible for $h\nu_{exc}$ exceeding 3.369 eV. Figures 2(a) and 2(b) show P_c (the open circles) as a function of detection energy ($h\nu_{det}$) measured from the Cermet and EaglePicher ZnO. Here, the PL was excited

at the energy that provides the maximum polarization in each sample, i.e. at $h\nu_{exc} = 3.3668$ and 3.3673 eV, respectively. For easy reference, also shown are PL spectra of these samples (the solid curves). Among all BX, a sizable PL polarization degree under such excitation conditions is only generated for the I^* and I_1^* excitons which implies that the observed resonance in the P_c ($h\nu_{exc}$) dependences should be related to the intrinsic energy structure of these IBX. This assumption is further confirmed by PL excitation (PLE) measurements performed on I^* and I_1^*. The corresponding PLE spectra are shown by solid dots in Figs. 2(c) and 2(d), respectively, and exhibit resonant enhancement at the same excitation energies as those required to generate P_c.

Let us now discuss the origin of the observed polarization. From Figs. 2(c) and 2(d), it is reasonable to suggest that the optical orientation of I^* (or I_1^*) by circularly polarized light is achieved under resonant excitation at a higher lying excited state (labeled as E_1) of this exciton located at around 4 meV above the ground state (labeled as E_0), as shown schematically in Fig. 2(e). The PL polarization degree is positive, i.e. the emitted light has an opposite helicity to the excitation light. This implies that the projection of the angular momentum of the IBX complex differs between its excited and ground states. According to our previous magneto-optical studies [16], the ground state of the I^* and I_1^* excitons is formed from electron and hole states with an effective spin 1/2. The electron wave function is s-like, i.e. $|\pm\frac{1}{2}\rangle_e$, whereas the hole component of the wave function is constructed as $|+\frac{1}{2}\rangle_h = -\gamma|+1,\Downarrow\rangle - \delta|0,\Uparrow\rangle$ and $|-\frac{1}{2}\rangle_h = \gamma|-1,\Uparrow\rangle + \delta|0,\Downarrow\rangle$. Here, $|+\frac{1}{2}\rangle_e (|-\frac{1}{2}\rangle_e)$ denotes the spin-up (spin-down) electron state, i.e. $|+\frac{1}{2}\rangle_e = |\uparrow\rangle (|-\frac{1}{2}\rangle_e = |\downarrow\rangle)$, and $|m_l,\Uparrow\rangle$ ($|m_l,\Downarrow\rangle$) denotes the hole state constructed from the orbital state $|m_l\rangle$ and spin-up (spin-down) spin state. The parameters γ and δ describe mixing of the $|m_l = \pm 1\rangle$ and $|m_l = 0\rangle$ states of the hole, with $\gamma^2 + \delta^2 = 1$ and $\gamma^2 \gg \delta^2$. This is to a certain extent similar to the A-VB hole states in ZnO, though the contribution from the $|m_l = 0\rangle$ state is significantly higher for the holes tightly bound at the isoelectronic I^* and I_1^* centers, likely due to combined effects of the spin-orbit interaction and local crystal field. The ground exciton state is fourfold degenerate and contains two bright states, i.e $|+\frac{1}{2}\rangle_h|+\frac{1}{2}\rangle_e$ and $|-\frac{1}{2}\rangle_h|-\frac{1}{2}\rangle_e$ that emit light in the σ^+ and σ^- polarization, respectively, and two dark states that are spin forbidden in optical transitions—see Fig. 2(e). The excited state of these excitons should then contain either p-like electron or $|+1,\Uparrow\rangle$ and $|-1,\Downarrow\rangle$ hole states, to account for the observed counter-polarization of the I^* and I_1^* emissions in the optical orientation experiments—see Figs. 2(a)–2(d). Since the electron within the BX complex is effective mass like [15], the former is highly unlikely. Indeed, the energy difference between the $1s$ and $2p$ states of the effective mass donor in ZnO is around 30–40 meV [17], i.e. by far too large to account for the 4.7 (3.2) meV energy separation between E_0 and E_1 of the $I^*(I_1^*)$ center. We, therefore, suggest that the E_1 state is constructed from the $|\pm\frac{1}{2}\rangle_e$ electron state and $|\pm\frac{3}{2}\rangle_h$ hole state (i.e. $|+1,\Uparrow\rangle$ and $|-1,\Downarrow\rangle$, possibly with some admixture of other hole states). This seems to indicate that the hole in the E_1 state couples to the B-VB states, which is in a way consistent with the energy separation between E_0 and E_1

that is very close to the A-B splitting. Resonant excitation of E_1 by the σ^--polarized light will generate population of the $|-\frac{3}{2}\rangle_h|+\frac{1}{2}\rangle_e$ state. If the generated electron spin orientation is preserved within the E_1 lifetime and during subsequent energy relaxation to E_0, this will in turn lead to the population of the bright $|+\frac{1}{2}\rangle_h|+\frac{1}{2}\rangle_e$ state of E_0 and thus positive P_c, as shown schematically in Fig. 2(e).

We also note that absorption of the circularly polarized light by FX_A does not generate spin polarization of either I^* or I_1^* excitons. This can be attributed to combined effects of fast spin relaxation of the free exciton [13] and spin loss during its capture by the isoelectronic centers.

B. Spin dynamics

The measured P_c values of time-integrated I^* and I_1^* emissions are relatively low, which suggest either incomplete electron spin generation at E_1 after the excitation process or spin loss at E_0 caused by spin relaxation. In order to achieve a better understanding of the IBX spin dynamics, we have performed time-resolved PL measurements under circularly (σ^-) polarized pulsed excitation which was tuned in resonance with the E_1 excited state. Representative decays of the PL polarization measured after the laser pulses at three different temperatures are shown in Figs. 3(a)–3(c) (the open circles), taking as an example the I^* emission. Also shown are decays of the total PL intensity ($I^+ + I^-$), represented by the solid lines. The decays of the PL polarization clearly contain several components which indicate involvement of different processes of optical depolarization. The first process, which is faster than the instrumental response of 10 ps, readily reduces the degree of PL polarization down to about 11% (at 4 K) for I^* and 13% for I_1^*. It is followed by a relatively fast P_c decrease within the first 400 ps after which the degree of PL polarization remains practically constant
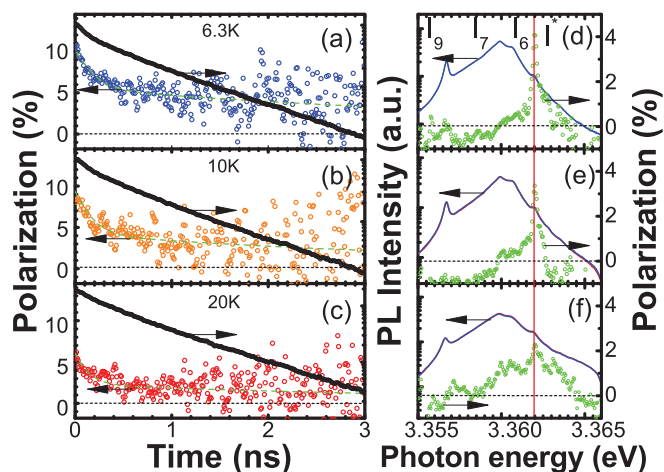

FIG. 3. (Color online) (a)–(c) Measured temporal decays of the total PL intensity (solid lines) and circular polarization (open circles) for the I^* emission at the specified temperatures. The dashed lines are just a guide to the eye to illustrate the P_c decays. (d)–(f) Photoluminescence spectra (solid lines) and $P_c(h\nu_{det})$ dependences that were time-integrated within the window of 2–5 ns after the end of the excitation pulse.

with further time delay Δt_d after the excitation pulse. The same temporal behavior of the PL polarization was observed for all measurement temperatures between 6.3 and 30 K, though the initial values of P_c continuously decreased at higher temperatures. Since the experimental data become rather noisy when Δt_d exceeds 2 ns, the existence of P_c in this temporal range was further confirmed by measuring P_c as a function of emission energy that were integrated within the time interval of $\Delta t_d = 2$–5 ns—see Figs. 3(d)–3(f). Undoubtedly, the I^* (and also I_1^*) emission remains circularly polarized within this time window, and the measured P_c corresponds to the values reached after the initial P_c decays depicted in Figs. 3(a)–3(c). From Fig. 3, it is also noticeable that the fast temporal decay of P_c coincides with the fast decay of the total PL intensity. The latter is found to be biexponential and to contain fast and slow decay components with the corresponding decay times of 0.18 and 0.75 ns, respectively. Though these time constants are found to be temperature independent within the range of 4–30 K, the contribution of the fast PL decay component decreases with increasing temperature.

The results of the performed transient PL and P_c measurements can be explained within two models which differ in interpretation of the biexponential character of the PL decay. The first model assumes that the fast component of this decay reflects spin dynamics of IBX and is caused by exciton transfer between the bright and dark states. Within the second model, on the other hand, two PL decay components are considered to simply stem from excitons recombining in two spatial regions with distinctly different carrier lifetimes such as surface and bulk areas of ZnO. Let us now discuss these models in more detail.

1. Model I

The fourfold degenerate ground state E_0 of the I^* and I_1^* excitons contains two bright and two dark states. The resonant optical excitation of the excitons at E_1 will populate the bright states of E_1 with the specific angular momentum that is allowed by the electric-dipole selection rule. After these E_1 excitons are optically generated, they will undergo population transfer between the sublevels of E_1 and, more significantly, energy relaxation down to the exciton ground state E_0. As it is reasonable to assume that the energy relaxation processes that conserve electron spin angular momentum should be more probable than the spin-flipping ones, it is expected that two of the four sublevels of E_0, namely the σ^+-active $|+\frac{1}{2}\rangle_h|+\frac{1}{2}\rangle_e$ and the dark $|-\frac{1}{2}\rangle_h|+\frac{1}{2}\rangle_e$, are more favorably fed from E_1 under the σ^- excitation [see Fig. 2(e)]. If the same applies to the hole spin during energy relaxation, the bright $|+\frac{1}{2}\rangle_h|+\frac{1}{2}\rangle_e$ is expected to be more populated than the dark $|-\frac{1}{2}\rangle_h|+\frac{1}{2}\rangle_e$. After the excitation pulses, populations of all four states within E_0 will start to equalize due to electron, hole, and exciton spin relaxation with characteristic time constants of τ_e^s, τ_h^s, and τ_{eh}^s, respectively—see Fig. 4(a). This could lead to the appearance of the biexponential PL decays, provided that spin relaxation time is shorter than the exciton lifetime. For a quantitative description of the spin and recombination dynamics at the exciton ground state, we resort to the following set of rate equations:
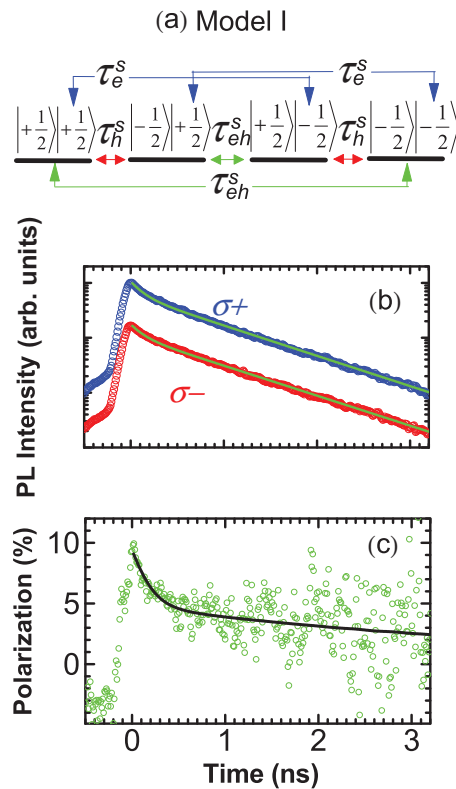
(a) Model I

FIG. 4. (Color online) (a) Schematic illustration of the spin-flip transitions in the exciton ground state E_0, which were considered in the rate equation analysis of the spin and recombination dynamics of the IBX. (b) Decays of the σ^+- and σ^--polarized I^* emission and (c) the corresponding PL circular polarization measured at 6.3 K under the σ^--polarized resonant excitation at the E_1 state. The open circles represent experimental data, whereas the solid lines are fitting curves based on model I, obtained using Eqs. (1)–(4) with the fitting parameters given in the text. The PL decays are vertically offset, for clarity.

$$\frac{dn_{++}}{dt} = -\frac{n_{++}}{\tau_r} + \left(\frac{n_{-+} - n_{++}}{\tau_h^s}\right) + \left(\frac{n_{+-} - n_{++}}{\tau_e^s}\right)$$
$$+ \left(\frac{n_{--} - n_{++}}{\tau_{eh}^s}\right), \quad (1)$$

$$\frac{dn_{-+}}{dt} = -\frac{n_{-+}}{\tau_r'} + \left(\frac{n_{++} - n_{-+}}{\tau_h^s}\right) + \left(\frac{n_{--} - n_{-+}}{\tau_e^s}\right)$$
$$+ \left(\frac{n_{+-} - n_{-+}}{\tau_{eh}^s}\right), \quad (2)$$

$$\frac{dn_{+-}}{dt} = -\frac{n_{+-}}{\tau_r'} + \left(\frac{n_{--} - n_{+-}}{\tau_h^s}\right) + \left(\frac{n_{++} - n_{+-}}{\tau_e^s}\right)$$
$$+ \left(\frac{n_{-+} - n_{+-}}{\tau_{eh}^s}\right), \quad (3)$$

$$\frac{dn_{--}}{dt} = -\frac{n_{--}}{\tau_r} + \left(\frac{n_{+-} - n_{--}}{\tau_h^s}\right) + \left(\frac{n_{-+} - n_{--}}{\tau_e^s}\right)$$
$$+ \left(\frac{n_{++} - n_{--}}{\tau_{eh}^s}\right). \quad (4)$$

Here, n_{++}, n_{-+}, n_{+-}, and n_{--} are exciton populations at the $|+\frac{1}{2}\rangle_h|+\frac{1}{2}\rangle_e$, $|-\frac{1}{2}\rangle_h|+\frac{1}{2}\rangle_e$, $|+\frac{1}{2}\rangle_h|-\frac{1}{2}\rangle_e$, and $|-\frac{1}{2}\rangle_h|-\frac{1}{2}\rangle_e$ sublevels of E_0, respectively. τ_r ($\tau_r^?$) represents the lifetime of the bright (dark) states. In the simulations, τ_r was set to 0.7 ns, i.e. to the value comparable with the decay time of donor bound excitons. It was also assumed that the hole relaxation time is shorter than that for the electron, as commonly observed in semiconductor materials. The best fit to the measured decays of the I^* intensity $I_{PL}(t)$ and its polarization $P_c(t)$ yields $\tau_r' = 0.9 \pm 0.05$ ns, $\tau_h^s = 0.4 \pm 0.05$ ns, $\tau_e^s = 15 \div 25$ ns, and $\tau_{eh}^s = 15 \div 30$ ns. The low accuracy in determining the τ_e^s and τ_{eh}^s values is due to the limited time range available for the analysis, which is restricted by the exciton lifetime. The simulated transients of the σ^+- and σ^--polarized PL components, as well as of $P_c(t)$ are shown by the solid lines in Figs. 4(b) and 4(c), respectively, together with the experimental data (the open circles) obtained under the σ^- excitation.

A comparable value of τ_h^s with that of the fast P_c decay indicates that the initial decrease of P_c is caused by hole spin relaxation, which transfers exciton population from the initially more populated $|+\frac{1}{2}\rangle_h|+\frac{1}{2}\rangle_e$ state to the $|-\frac{1}{2}\rangle_h|+\frac{1}{2}\rangle_e$ state until they reach a dynamical balance between them. In contrast, the processes involving electron and exciton spin flips, see Fig. 4(a), are much longer than the exciton lifetime. This gives rise to a nearly constant value of P_c for time delays exceeding 0.6 ns.

Model I can also explain the results from the temperature-dependent measurements shown in Fig. 3. The decays of both PL intensity and its circular polarization can be reproduced assuming temperature-independent values of all time constants. The decreasing contribution of the fast decay components at higher temperatures can be attributed to a decrease in the population difference between the bright and dark states immediately after the end of the excitation pulse, i.e. at $\Delta t_d = 0$. This in turn means acceleration of the spin relaxation during the feeding process, i.e. either at the excited E_1 state or/and during the energy relaxation from E_1 to E_0. This accelerated spin loss can also explain the observed decrease in the initial P_c value (i.e. at $\Delta t_d = 0$) with increasing measurement temperature, as this process should equalize populations of two bright states of E_0 either via subsequent electron and hole spin flips or via direct exciton spin-flip.

2. Model II

Our previous transient study of D^0X [21] has shown that these transitions in ZnO often exhibit a biexponential decay which reflects contributions of exciton emissions from two spatial regions with distinctly different exciton lifetimes, i.e. close to the surface (short lifetime) and in bulk (long lifetime). In model II, it is assumed that the same could be true for the isoelectonic I^* and I_1^* excitons, such that the observed PL decay is a superposition of the two contributions, i.e.

$$I_{PL} = A_f \exp\left(-\frac{t}{\tau_f}\right) + A_s \exp\left(-\frac{t}{\tau_s}\right). \quad (5)$$

Here, A_f (A_s) denotes the amplitude of the surface-related fast (bulk-related slow) component with the time constant of τ_f (τ_s). In the case of D^0X, the ratio between A_f and A_s depends
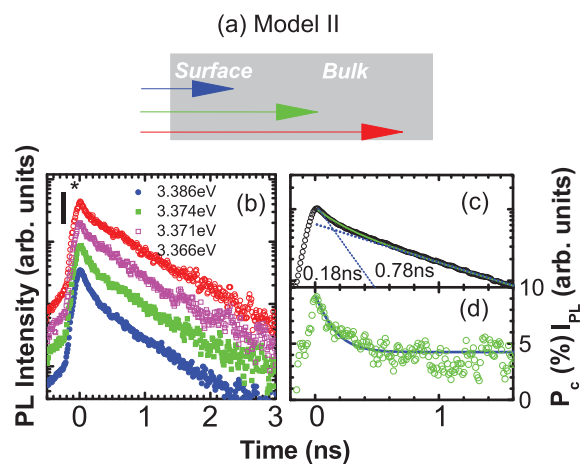

FIG. 5. (Color online) (a) Schematic illustration of relative contributions of the surface-related and bulk emissions with respective to the excitation energy and thus the penetration depth of the excitation light. (b) Decays of the total intensity of the I^* emission measured at 6.3 K using different excitation energies of linearly polarized light. (c) Decay of the total intensity of the I^* emission measured at 6.3 K under excitation with linearly polarized light tuned in resonance with the E_1 state (the open circles). The dotted lines are fitting curves using Eq. (5). (d) Decay of the I^* circular polarization measured at 6.3 K under the σ^--polarized resonant excitation at the E_1 state (the open circles). The solid line is a fitting curve obtained based on model II.

on the excitation energy ($h\nu_{exc}$) due to variations in penetration depth of the laser light [21]—see Fig. 5(a). The contribution of the surface-related recombination continuously decreases when the excitation energy is tuned below FX_A and is moved farther away from it. To verify whether the same behavior is also observed for the isoelectronic bound excitons, PL decays of I^* were measured under different $h\nu_{exc}$. The corresponding results are shown in Fig. 5(b) and show the same trend of decreasing A_f with increasing $h\nu_{exc}$ as was observed for D^0X. This finding, therefore, is consistent with the suggestion that the fast component of the PL transient reflects the I^* lifetime in the near-surface region. (We cannot rule out model I based on this finding, however, as a change in $h\nu_{exc}$ may also result in different populations of the dark and bright states of E_0 and, therefore, affect the relative contribution of the fast PL decay.) Using model II, the measured decays of the PL intensity and polarization can be reproduced assuming that $\tau_f = 0.18 \div 0.02$ ns, $\tau_s = 0.75 \div 0.03$ ns, and that P_c remains constant within the PL lifetime, as demonstrated in Figs. 5(c) and 5(d) by a comparison between the simulation (the solid lines) and experimental data (the open circles) measured at 6.3 K for the I^* emission. The P_c values of the fast and slow component were kept constant in time and equal to 20 and 4%, respectively. We note that, in order to reproduce the experimental data, the P_c value needs to be significantly higher for the fast PL component. Though such a large difference in the P_c values is somewhat surprising, it could in principle be attributed to a shorter lifetime of the exciton and consequently a reduced contribution of spin relaxation in the near-surface region as compared with the bulk region. Based on Eqs. (1)–(4), the constant P_c in time implies

that the characteristic times of all spin-flip processes (i.e. for the electron, the hole, and the exciton as a whole) are longer than the exciton lifetimes with the low bound of 10 (15) ns for the near-surface (bulk) regions. An overall decrease of the PL polarization with rising temperature (Fig. 3) can be ascribed to the temperature-induced acceleration of spin relaxation during the feeding process, i.e. similarly to model I. Model II faces difficulties, however, when explaining the suppression of the fast PL decay component at elevated temperatures. Indeed, contributions of the surface-related and bulk $I^*(I_1^*)$ excitons under resonant excitation via the E_1 state are expected to be solely determined by the penetration depth of the excitation light, which is temperature independent. This makes this model somewhat less likely.

We, therefore, suggest that, though surface effects may contribute to the spin dynamics, the main physical process responsible for the appearance of the fast decay component in the I^* and I_1^* transients is the spin relaxation from the bright to dark state within the exciton ground state accomplished via a hole spin-flip. The same process also leads to the initial decay of the circular PL polarization in optical orientation experiments.

C. Origin of spin relaxation

Let us now briefly discuss spin relaxation processes that govern spin dynamics of the studied isoelectronic bound excitons in ZnO. We can first examine the determined time constants of the spin-flip transitions at the exciton ground state. The fastest process is spin relaxation of the bound hole with τ_h^s equal to 0.4 ns. Though being relatively short, this value is still longer than the spin-flip time of an effective-mass hole bound within the D^0X complex, i.e. 100 ps in bulk ZnO [13]. The observed slow-down of the hole spin relaxation is probably not surprising as partial quenching of the orbital angular momentum for the tightly bound hole should weaken spin-orbit interaction that usually dominates hole spin dynamics. On the other hand, electron spin relaxation is significantly slower, i.e. 15 ns or longer at $T < 30$ K. This is likely a result of localization at the isoelectronic center which deactivates spin relaxation mechanisms related to carrier motion, such as Dyakonov-Perel [7] or Elliot-Yafet processes [8,9]. The determined value of τ_e^s is in fact comparable with the spin coherence time of an electron bound to an effective-mass donor in ZnO (25 ns) that was concluded to be limited by the hyperfine interaction with nuclear spins of the naturally occurring ^{67}Zn isotope [11]. Moreover, our results show that direct spin relaxation between the bright states via an exciton spin-flip is also a rather slow process characterized by $\tau_{eh}^s \geqslant 15$ ns. We suggest that this reflects combined effects of a weak e-h exchange interaction for the studied IBX [16] and exciton localization. The latter should diminish importance

of the long-range e-h exchange interaction, which has been shown to dominate spin relaxation of free excitons but weakens linearly with decreasing momentum K [22].

From Fig. 3, the initial value of the exciton polarization generated at E_0 by optical orientation is rather low. As a reminder, this optical orientation is believed to be accomplished via the resonant excitation at the higher lying excited state (E_1) of the isoelectronic BX. The low initial value of P_c could, therefore, be caused by two factors. First of all, it can reflect poor generation of spin polarization at E_1 if the states forming E_1 are spin mixed. Though the exact structure of the E_1 state could not be determined from the present study, this is very likely as spin mixing (though weak) is known to occur in the exciton ground state. Secondly, it can be a result of fast spin relaxation during the feeding process, i.e. spin loss at E_1 prior to and during the energy relaxation to E_0. The contribution of these processes becomes more significant at temperatures exceeding 10 K, since raising temperature causes a decrease in the initial P_c values. This thermally accelerated spin relaxation can be caused by, for example, the Orbach-type relaxation process [23].

IV. SUMMARY

In conclusion, we have employed the time-resolved optical spin orientation technique to study spin dynamics of I^* and I_1^* excitons bound to isoelectronic centers in bulk ZnO single crystals. We show that spin orientation at the exciton ground state E_0 can be generated using resonant excitation at a higher lying exciton state located at about 4 meV apart from E_0. The induced circular PL polarization declines within the first 400 ps after the end of the excitation pulse but remains practically constant with further time delay. The rate equation analysis of the observed spin dynamics at the exciton ground state, which takes into account subsequent hole and electron spin flips between the bright and dark states of BX and direct exciton spin flips between the bright states of E_0, allows us to determine the characteristic time constants of these processes as being $\tau_h^s = 0.4$ ns, $\tau_e^s \geqslant 15$ ns, and $\tau_{eh}^s \geqslant 15$ ns, respectively. These values are substantially longer than spin relaxation times for a free exciton (<10 ps) or an effective-mass hole bound to a donor-bound exciton complex (0.1 ns) that were determined previously in bulk ZnO [13]. The slowdown of the exciton spin relaxation likely reflects combined effects of exciton localization at the isoelectronic center and a weak exchange interaction of the studied BX. The relatively slow hole spin relaxation in IBX can be attributed to the suppressed spin-orbit coupling for the tightly bound hole. Our findings, therefore, indicate that this class of bound excitons is attractive for applications in spin-functional light emitters.

[1] Ü. Özgür, Y. I. Alivov, C. Liu, A. Teke, M. A. Reshchikov, S. Doğan, V. Avrutin, S.-J. Cho, and H. J. Morkoc, J. Appl. Phys. **98**, 041301 (2005).

[2] C. Klingshirn, Phys. Status Solidi B **244**, 3027 (2007).

[3] S. J. Pearton, D. P. Norton, M. P. Ivill, A. F. Hebard, J. M. Zavada, W. M. Chen, and I. A. Buyanova, IEEE Trans. Electron Devices **54**, 1040 (2007).

[4] T. Dietl, H. Ohno, F. Matsukura, J. Cibert, and D. Ferrand, Science **287**, 1019 (2000).

[5] S. J. Pearton, D. P. Norton, Y. W. Heo, L. C. Tien, M. P. Ivill, Y. Li, B. S. Kang, F. Ren, J. Kelly, and A. F. Hebard, J. Electron. Mater. **35**, 862 (2006).

[6] S. Chambers, T. Droubay, C. Wang, K. Rosso, S. Heald, D. Schwartz, K. Kittilstved, and D. Gamelin, Mater. Today **9**, 28 (2006).

[7] M. I. Dyakonov, *Spin Physics in Semiconductors* (Springer, New York, 2008).

[8] R. Elliott, Phys. Rev. **96**, 266 (1954).

[9] Y. Yafet, in *Solid State Physics*, edited by F. Seitz, D. Turnbull (Academic, New York, 1963), Vol. 14.

[10] S. Ghosh, V. Sih, W. H. Lau, D. D. Awschalom, S.-Y. Bae, S. Wang, S. Vaidya, and G. Chapline, Appl. Phys. Lett. **86**, 232507 (2005).

[11] H. Horn, A. Balocchi, X. Marie, A. Bakin, A. Waag, M. Oestreich, and J. Hubner, Phys. Rev. B, **87**, 045312 (2013).

[12] W. K. Liu, K. M. Whitaker, A. L. Smith, K. R. Kittilstved, B. H. Robinson, and D. R. Gamelin, Phys. Rev. Lett. **98**, 186804 (2007).

[13] D. Lagarde, A. Balocchi, P. Renucci, H. Carrère, F. Zhao, T. Amand, X. Marie, Z. X. Mei, X. L. Du, and Q. K. Xue, Phys. Rev. B **78**, 033203 (2008).

[14] W. M. Chen, I. A. Buyanova, A. Murayama, T. Furuta, Y. Oka, D. P. Norton, S. J. Pearton, A. Osinsky, and J. W. Dong, Appl. Phys. Lett. **92**, 092103 (2008).

[15] I. A. Buyanova, A. Murayama, T. Furuta, Y. Oka, D. P. Norton, S. J. Pearton, A. Osinsky, J. W. Dong, C. W. Tu, and W. M. Chen, J. Supercond. Novel Magn. **23**, 161 (2010).

[16] S. L. Chen, W. M. Chen, and I. A. Buyanova, Phys. Rev. B **86**, 235205 (2012).

[17] B. K. Meyer, J. Sann, S. Eisermann, S. Lautenschlaeger, M. R. Wagner, M. Kaiser, G. Callsen, J. S. Reparaz, and A. Hoffmann, Phys. Rev. B **82**, 115207 (2010).

[18] B. K. Meyer, H. Alves, D. M. Hofmann, W. Kriegseis, D. Forster, F. Bertram, J. Christen, A. Hoffmann, M. Straßburg, M. Dworzak, U. Haboeck, and A. V. Rodina, Phys. Status Solidi B **241**, 231 (2004).

[19] S. L. Chen, W. M. Chen, and I. A. Buyanova, Appl. Phys. Lett. **99**, 091909 (2011).

[20] D. G. Thomas, J. Phys. Chem Solids **15**, 86 (1960).

[21] S. L. Chen, W. M. Chen, and I. A. Buyanova, Appl. Phys. Lett. **102**, 121103 (2013).

[22] M. Z. Maialle, E. A. de Andrade e Silva, and L. J. Sham, Phys. Rev. B **47**, 15776 (1993).

[23] C. B. P. Finn, R. Orbach and W. P. Wolf, Proc. Phys. Soc., (London) **77**, 261 (1961).